DOR: 20.1001.1.25383620.2021.5.2.5.1

Studies on the Microstructure Modification and Tribological Characteristics of Cast Al-Si Eutectic Alloys

V. Abouei Mehrizi[1,*], O. Bayati[2]

[1]Advanced Materials Engineering Research Center, Karaj Branch, Islamic Azad University, Karaj, Iran.
[2]Department of Metallurgy and Materials Engineering, Hamedan University of Technology, Hamedan, Iran.
Received 24 July 2021 - Accepted: 20 *November 2021*

Abstract

The focused of this investigation is on the modification of Fe-rich intermetallics morphology and wear and friction properties of eutectic Al-Si alloys. Eutectic Al-Si specimens were fabricated by tilt casting technique after addition of different amounts of iron and manganese to the melt alloy. Dry sliding tribological behavior of the samples were investigated using a reciprocating wear tester at the room temperature in atmospheric environment. It is found that the addition of iron up to 1.5 wt.pct to the alloy decreased the wear resistance of alloy owing to the formation of brittle plate-like β-Al_5FeSi intermetallic compounds. As Manganese is added to the β-containing alloy up to the half of iron content (corresponding to a Mn/Fe ratio of 0.5), the platelet phases are completely replaced by the star-like α-$Al_{15}(Fe,Mn)_3Si_2$ intermetallics resulting in improved wear resistance of the alloy. Introducing 0.8 wt.pct Mn to the alloy containing 1.6 wt.pct Fe did not convert the plate-like beta intermetallics to the modified alpha compounds completely and had no impressive impact on the wear rate of the alloy.

Keywords: Eutectic Aluminum-Silicon Alloys, Intermetallic Morphologies, Mn Modifier, Friction Coefficient.

1. Introduction

Studies on the tribological behaviors of Al-Si alloys have been proved that various material-related factors such as mechanical properties, microstructure and practical conditions could effect on the wear and friction characteristics of the alloys [1-4]. Unique features of eutectic and hypereutectic Al-Si casting alloys such as privileged wear properties, low coefficient of thermal expansion (CTE), high corrosion resistance, high strength to weight ratio, excellent castability and low cost have been made them as an interesting materials for the engine blocks, diesel engine crankcases, cylinder heads, pistons, gasoline and oil tanks, water cooled cylinder heads, typewriter frames, rear axle housing and engine parts [5-9]. Over the last decade, several attempts were performed in order to achieve modified microstructure and superior wear resistance as an applied property in Al-Si alloys [10-14]. Also, many researches were conducted to design and produce new resisting materials in order to control and decrease the wear rate and coefficient of friction in various conditions [15-19]. Chemical modification and refinement of the microstructure, rapid solidification technique, semi-solid process, spray forming, heat treatments, utilization of various coatings and surface treatments are the common processes used in this field [11,17-20] The addition of iron to the eutectic Al-Si alloys, although lead to precipitation of detrimental β-Al_5FeSi intermetallics, can improve high temperature properties and thermal stability of the alloy [21,22].

[*]Corresponding author
Email address: vahid.abouei@kiau.ac.ir

Efforts have to be made to modify the harmful influences of Fe-rich compounds, e.g., by refining their size and by modifying them to the less deleterious morphologies. Nevertheless, investigations on the addition of grain refiner and modifier to the microstructure and their effects on the tribological behaviors have not yet been explored extensively. In a recent study [23] we concluded that the addition of iron to the hypereutectic Al-Si alloys can form Fe-rich intermetallic compounds such as β-Al_5FeSi and δ-$Al_4(Fe,Mn)Si_2$. These phases present as needle-like and cubic structures and although increase the hardness result in poor wear properties. Investigations have shown that the morphology of needle-like and flake-like iron-rich compounds could be modified by adding some proper elements such as Mn, Cu, Mg, Cr, Co, B, Sn and Sr [24-28]. Hekmat-Ardakan et al. [29] have shown that Mg addition to the Al-17%Si alloy could modify the microstructure of the alloy. In another study, it was reported that the addition of Sn to the hypereutectic A390 alloy changed the microstructure and reduce the wear rates and friction factors of alloys [30]. It has been shown that the addition of Mn to the hypereutectic Al-Si alloys modifies the needle-like morphology of Fe-rich intermetallics into the star-like compounds and declines the wear rate of the alloy [23]. In the present study an attempt was made to investigate the modification of intermetallic compounds morphology of eutectic Al-12.5Si alloy through addition of manganese and

dry reciprocating wear and friction characteristics of the alloy.

2. Materials and Methods

In Table. 1. are listed the chemical composition of eutectic Al-Si alloys used in the present study. In order to investigate the effects of Fe-rich intermetallics and Mn addition on the microstructure and wear behavior of the alloy, iron and manganese were added to the base alloy in order to obtain 1Fe alloy containing 1 wt.% Fe, 1FeMn alloy containing 1 wt.% Fe and 0.5 wt.% Mn and 1.6FeMn alloy containing 1.6 wt.% Fe and 0.8 wt.% Mn. Iron and Manganese were added to the melt at 750 °C using ALTAB Fe Compact (75 wt.% Fe, 15 wt.% Al and 10 wt.% nonhygroscopic Na-free flux) and Mn compact (75 wt.% Mn, 15 wt.% Al, and 10 wt.% nonhygroscopic Na-free flux), respectively. The composition of the samples was done by spark emission spectrometry by FOUNDRYMASTER Smart machine. After addition of Fe and Mn, The temperature of the melt was raised to 800 °C, held for 15 min to homogenize the liquid and then cooled in the furnace to 750 °C. The melt was stirred and degassed using Foseco 600 tablet for 10 min before pouring. Final pouring temperature was always 720 ± 5 °C. The molten alloys were cast into a copper mold having the average cooling rate of 7.5 °C s^{-1}. The hardness of all samples was measured according to the ASTM E92 standard using a Brinell hardness tester with the load of 31.25 kgf. The effect of alloy chemistry on the microstructure was studied using scanning electron microscopy (SEM: FEI ESEM QUANTA 200) attached with energy dispersive X-ray analyses (EDS) and X-ray diffraction (XRD). The volume fraction of the Fe-rich intermetallic was related to the area fraction which was measured by the quantitative metallography using a computer-assisted Buhler Omnimet image analysis system. Reciprocating wear was carried out at a relative humidity of 40 ± 2% at room temperature (25 °C) against the counterface of a hardened and polished steel disk with HRC 64 hardness. The cylindrical pins, 5 mm in diameter and 25 mm in height, were in a conformal contact with the disk. The wear tests according to ASTM G99 standard, were conducted under nominal loads of 21, 48, 75 and 98 N, at a constant sliding speed of 0.45 ms^{-1} for a sliding distance of 1000 m. Each test was repeated three times at a given load and sliding velocity.

3. Results and Discussion

3.1. Microstructures and Hardness

The microstructure of the base alloy is displayed in Fig. 1. It contains some Fe-rich, Ni and Cu-rich intermetallics due to the presence of Fe, Ni and Cu in the composition of alloy (phase A and B). Each intermetallic phase has been analyzed three times in the sample and the average chemical composition of the intermetallics is given in Table. 2. Fig. 2. shows the microstructural features of the eutectic alloys having different amounts of iron and manganese

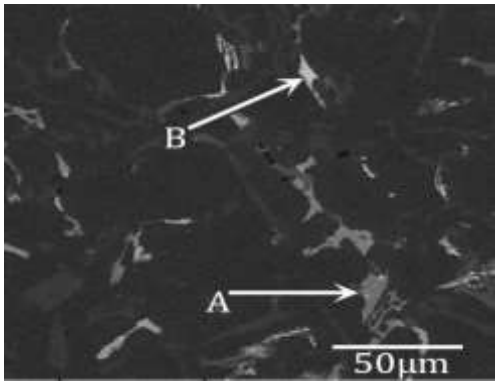

Fig. 1. Microstructure of the base alloy containing Ni-rich (gray) and Cu-rich (white) Intermetallics.

(Table. 1.). The addition of iron to the base alloy led to the precipitation of plate-like intermetallic phases in the matrix as shown in Fig. 2.a (β phase). The average atomic concentrations of Al, Fe and Si were in good agreements with the concentrations obtained for the β-Al_5FeSi flakes by others [31-33]. Fig. 2.b shows the microstructure of 1FeMn alloy. The addition of Mn up to the half of Fe amount causes the replacement of β-plate-like intermetallic by the star-like and sometimes branched morphologies (α phase).

Table. 1. Designations and chemical compositions of the eutectic alloys (wt.%).

Alloy code	Si	Cu	Ni	Mg	Zn	Fe	Mn	Al
Base	12.53	1.08	1.17	0.97	0.01	0.43	--	Balance
1Fe	12.61	0.86	0.94	0.96	0.01	1.02	--	Balance
1FeMn	12.79	1.11	1.07	0.92	0.01	0.99	0.51	Balance
1.6FeMn	12.58	0.79	1.03	0.94	0.01	1.56	0.79	Balance

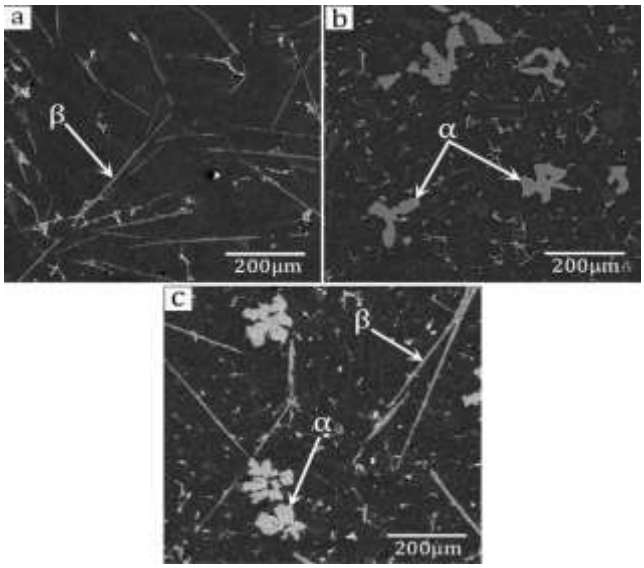

Fig. 2. Microstructures of the (a) 1Fe alloy, (b) 1FeMn alloy and (c) 1.6FeMn alloy.

Table. 2. Chemical composition (wt.%) of the intermetallic compounds of the base alloy.

Phase designation/Chemical composition	Al	Si	Fe	Cu	Ni
Gray (A)	62.350	21.010	12.730	--	4.890
White (B)	70.220	0.610	11.190	10.380	8.540

Table. 3. Chemical composition of the phases shown in the micrographs of Fig. 2 (at.%).

Alloy Code	Phases	Morphology	Atomic percentage					
			Al	Si	Fe	Mn	Cu	Ni
1Fe	**α**	**Plate-like**	66.14**0**	13.59**0**	14.28**0**	--	--	--
1FeMn	**β**	**Star-like**	71.14**0**	10.03**0**	9.39**0**	7.76**0**	--	0.19**0**
1.6FeMn	**α**	**Plate-like**	67.78**0**	18.65**0**	11.25**0**	3.47**0**	--	0.85**0**
	β	**Star-like**	72.44**0**	10.37**0**	10.09**0**	6.71**0**	--	0.39**0**

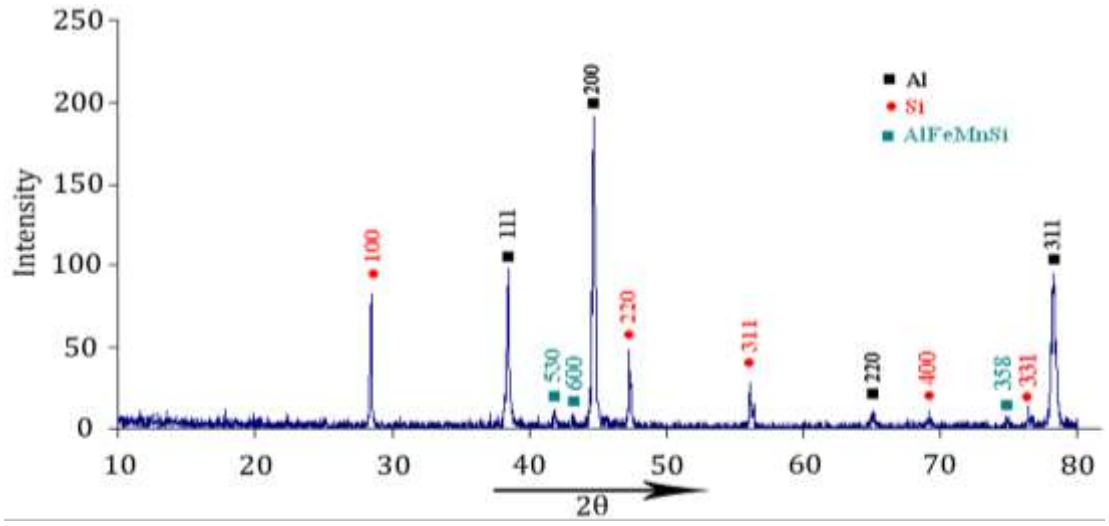

Fig. 3. The XRD pattern of the intermetallic obtained from the 1FeMn alloy.

The average atomic percentage of the elements in these intermetallics indicates that they are $Al_{15}(Fe,Mn)_3Si_2$ phases (Table. 3.). Fig. 2.c shows the effect of 1.6 wt.% Fe and 0.8 wt.% Mn addition on the microstructure of 1.6FeMn alloy.

As can be observed, exceeding amount of iron up to 1.6% in the 1.6FeMn alloy despite the presence of manganese leads to the formation of plate-like intermetallics adjacent to star-like compounds (β and α phases).

Table. 4. Hardness, volume fraction and average maximum size of Fe-rich intermetallics phases.

Alloy Code	Hardness (HB)	Volume Fraction of Phase (%)	Average Maximum Size of Phase (µm)
base alloy	84 ± 0.80	53.52 ± 21.22	-
1Fe	92 ± 0.35	6.57 ± 3.15	54.62 ± 2.81
1FeMn	93.5 ± 0.61	6.97 ± 3.59	31.32 ± 14.95
1.6FeMn	117 ± 0.92	(β) 4.61 ± 0.54	83.22 ± 39.62
		(α) 5.52 ± 1.29	32.07 ± 14.52

Chemical composition analysis of these compounds indicated β-Al_5FeSi and α-$Al_{15}(Fe,Mn)_3Si_2$ phases in the microstructure. Fig. 3. indicates XRD pattern of the 1.6FeMn alloy. As it is observed, in addition to Al and Si peaks, AlFeMnSi intermetallic compound peaks are depicted. Of course it should be taken into granted that considering the fact of not having access to standard diffraction patterns of intermetallic compounds observed in this work, defined peaks in Fig. 3. does have some percentage of margin of error (phase identification and indices has been performed according to Xpert software and reference [34]). Table. 4. presents the hardness of the alloys. It is observed that the hardness of the as-cast alloy shows an enhancement as the iron content of the alloy increased. As can be noticed, higher addition of Fe and Mn results to an increment in the hardness of 1.6FeMn alloy. The image analysis results of the volume fraction and the average of the maximum size of the intermetallics are presented in Table. 4. By increasing iron and manganese in 1.6FeMn alloy the size of alpha iron-rich intermetallics were increased and the volume fraction of them were decreased comparing to 1FeMn alloy, while the size of beta phases were increased 29% comparing to 1Fe alloy.

3.2. Wear Characterizations

The wear rate of the base alloy, 1Fe, 1FeMn and 1.6FeMn alloys at different applied loads of 21, 48, 75 and 98 N are compared with each other in Fig. 4. It can be observed that the addition of about 1% Fe to the base alloy creates a damaging effect on the wear behavior of the alloy. Also, the 1Fe alloy has the lowest wear resistance compared to the base alloy at all applied loads. Based on Fig. 4., the addition of Mn to the 1Fe alloy declines the harmful influences of iron and improves the wear rate of 1FeMn alloy compared to that of 1Fe alloy.
It can be seen that the addition of 0.8% Mn to the 1.6Fe alloy does not decrease the deleterious effects of iron, and consequently it does not have impressive effect on the wear rate of 1.6FeMn alloy compared to that of 1FeMn. In eutectic Al-Si alloys containing 11% silicon and higher, the presence of approximately more than 1.5% Fe despite the presence of manganese leads to the formation of plate-like Al_5FeSi intermetallic compounds, and thus, further Mn addition to alloy composition cannot prevent the formation of beta intermetallic compounds and decrease the deleterious effects of iron [35].

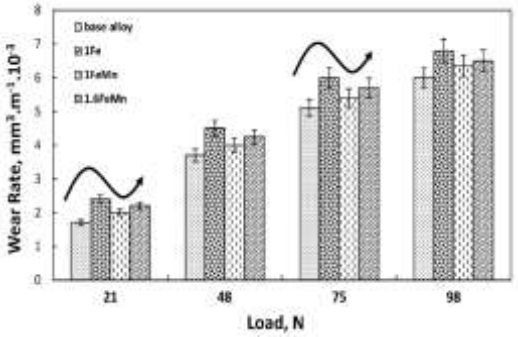

Fig. 4. Variation of wear rate versus applied load for different alloys.

The lower wear resistance of the 1.6FeMn alloy compared to the 1FeMn alloy is due to existence of plate-like intermetallic compounds and more potential to formation of microcracks in the subsurface of the alloy. SEM micrographs of the worn surface of the 1FeMn alloy under applied load of 98 N are shown in Fig. 5. Fig. 5.a shows that the worn surface was mostly covered by oxide particles.

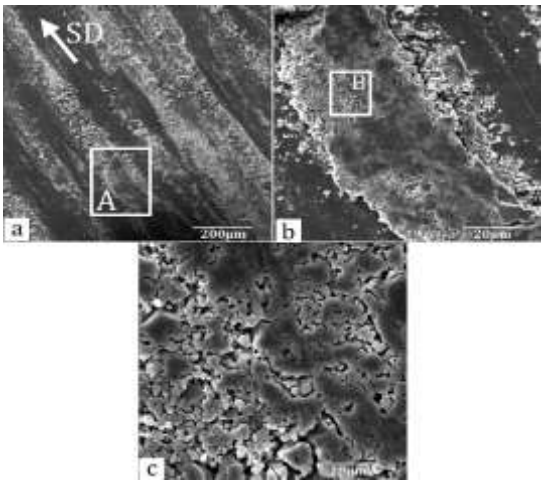

Fig. 5. SEM micrographs of worn surface of a) 1FeMn alloy at applied load of 98 N, b) enlarged view of the marked region (A) in the micrograph a, c) enlarged view of the marked region (B) in the micrograph b, (*SD is sliding direction).

The oxide particles formed on the overall worn surface of the pin contained a certain amount of iron, aluminium and oxygen as examined by EDS in Fig. 6. These debris could entrapped between the sliding surfaces and gets compacted due to the repetitive sliding and forms a tribolayer over the surface, as shown in 5b and c.

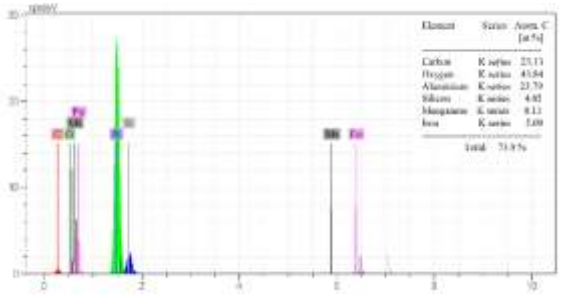

Fig. 6. EDS result of the worn surface of 1FeMn alloy at the applied load of 98 N.

The composition of the tribolayer formed on the overall worn surface of the pin has been presented in Fig. 6., Fig. 7.a shows the subsurface micrographs of base alloy subjected to an applied load of 48 N. Sliding high tangential stresses that occur on and below the sliding surface, result in nucleation of cracks within the plastically deformed material beneath the surface. The cracks can be propagated and their connection to each other can lead to fracture of metallic and intermetallic particles from the surface [36, 37].

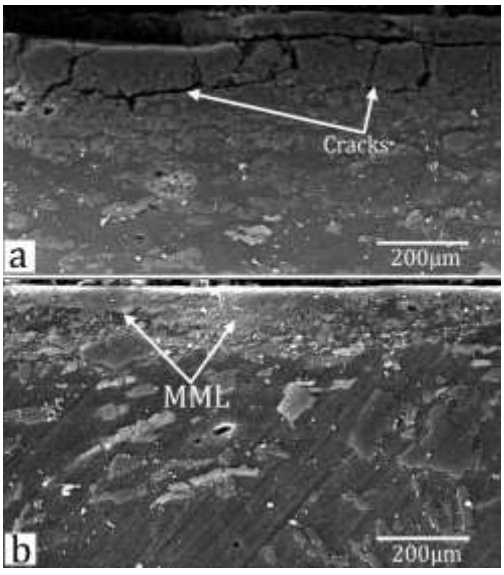

Fig. 7. Longitudinal cross-section of the worn surface of a) base alloy at the applied load of 48 N, b) 1FeMn alloy at the applied load of 98 N.

These fragmented metallic particles could be mechanically mixed with the oxides in the contact zone and form a tribolayer (MML) as shown in Fig. 7.b. The tensions derived on the surface during sliding, can weaken the tribolayer and lead to the delamination and fracture of oxide film generated through the wear debris as shown in Fig. 8. According to Fig. 9., the composition of the wear debris contained a certain amount of iron, aluminium and oxygen that is similar to what can be observed from the worn surfaces in Fig. 6. Decrease in the wear properties of 1Fe alloy compared to the base alloy, as shown in Fig. 4., can be explained based on the microstructural features of the alloys. Fig. 2.a shows that addition of iron to the base alloy led to the precipitation of β-phase intermetallic in the matrix. β-Al_5FeSi plate-like intermetallics are hard and brittle phases.

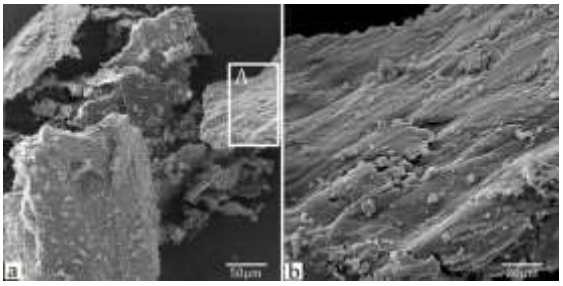

Fig. 8 a) SEM micrographs of wear debris of 1FeMn alloy at the applied load of 98 N, (b) enlarged view of the marked region (A) in the micrograph (a).

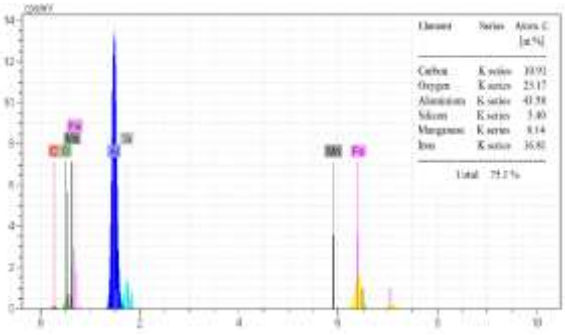

Fig. 9 EDS result of the wear debris of 1FeMn alloy at the applied load of 98 N.

They exist as discrete particles with a highly faceted nature in the alloy matrix [38]. Accordingly, it has relatively low bond strength with the matrix and the interfacial regions between this phase and the matrix become quite prone to microcracking [22, 39, 40]. Moreover, sharp edges of the β-plates introduce severe stress concentration effect into the alloy's matrix [41]. According to Fig. 4., the enhancement in the wear properties of 1FeMn alloy compared to 1Fe can be originated from the replacement of β-plate-like intermetallics by the modified α-intermetallic compounds. Since the α-intermetallics have a modified morphology rather than the β phase, they have little effect on the formation of surface and subsurface microcracks.
Also, the α-intermetallics form a rough interface with the matrix and their better bonding with the matrix declines the possibility of crack formation in

the interface of the intermetallic compounds with the matrix. Fig. 2.c shows that the addition of manganese to the 1.6Fe alloy led to the formation of α-phase intermetallic in neighboring β-phase in the matrix. The platelet nature of beta intermetallic compounds decreased wear resistance of the 1.6FeMn alloy, but its wear rate diminished compared to the 1Fe alloy. This phenomenon may have occurred due to hardness enhancement as a result of the formation of more volume fraction of intermetallic compounds. As, equality of proportion of wear rate in the 1.6FeMn alloy in comparison with the 1Fe alloy, shows decline of negative effects of intermetallic compounds, even in the case of presence of platelet intermetallic compounds in the alloy. According to Table. 3., the hardness of the alloys from base one to 1.6FeMn alloy illustrates linear increase, whereas wear rate of the alloys from base one to 1.6FeMn alloy follows approximately a sinusoidal procedure that its climax occurs in 1Fe alloy as shown in Fig. 4. This implies, although hardness values are effective on the wear resistance of eutectic Al-Si alloys, microstructure and morphology resulted from the chemical composition, play substantial role on the wear resistance of eutectic Al-Si alloys. According to Fig. 2.c the addition of 1.6% Fe and 0.8% Mn to the base alloy led to increasing of the wear rate of 1.6FeMn alloy. The reason for this is mainly due to stress concentration enhancement and crack formation as a result of the presence of plate-like intermetallic compounds [21]. Increasing percentage of iron to about 1.6% led to the formation of plate-like intermetallics adjacent to star-like particles and this issue due to stress concentration and tendency of plate-like particles to microcracking would resulted in decrease of wear resistance in the alloy.

Lowering wear resistance of eutectic alloys containing intermetallic compounds, in addition to alloy trend to crack formation and fracture and segregation of intermetallic compounds, can be considered as alloy brittleness increment owing to intermetallic compounds formation in the alloy structure.

3.3. Friction Coefficient

The variations of friction coefficient with sliding distance of the 1FeMn alloy under normal loads of 21 N and 98 N are shown in Fig. 10.a and Fig. 10.b. It is noted that the obtained friction coefficient curves are divided into two separated stages. These comprise of stage I: low friction stage (distances from 0 to 300 m) and stage II: high friction stage (distances longer than 300 m). In stage I, the friction coefficient has a low value and stable fluctuation that is most probably relevant to the oxide layer formation and prevention of metal-metal contact during sliding. With starting wear and consequently rising in temperature of worn surfaces, atmospheric oxidation of trapped metallic particles occurs and form a thin oxide layer between the sample and the counterface, so preventing direct metal-metal contact.

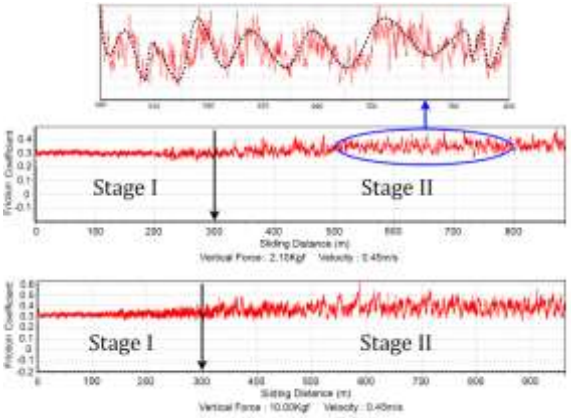

Fig. 10. Variation of friction coefficient with sliding distance of the 1FeMn alloy a) at the load of 21 N and b) at the load of 98 N.

The prevention of direct metal-metal contact that is owing to the reduction in adhesion of metallic surfaces and lubricating property of the oxide layer, led to the decrease of the friction coefficient. In stage II, with the increase in sliding distance, the friction coefficient increases and destabilizes.

As sliding continues, sliding mechanical stresses lead to instability and removal of the initial protective oxide layer. After the removal of oxide layer from surface, adhesion between the pin and the disk increases significantly. Under these conditions, due to the increment of pin temperature, hardness and strength of the subsurface is dropped and the tribolayer gets destabilized. Thus the metal-metal contact between surface alloy and steel disk is established and the friction coefficient increases.

The continuing process between the removal of oxide layer and its reformation could result in higher value and fluctuation of the friction coefficient of pin material. As it is obvious from Fig. 10.a and Fig. 10.b, at 21 N load, the friction coefficient in stage II has stabilized and alternating fluctuation, whereas the friction coefficient at the applied load of 98 N shows irregular and more fluctuations in the same conditions. Fig. 10.a, also illustrates the accurate investigation of friction curve at the distances in a range between 500 m and 800 m. As can be seen, the friction coefficient in these intervals comprises periodic minimum and maximum values almost after every few meters which can be attributed to consecutive adhesion and removal phenomenon of tribolayer. According to the obtained results, it is found that by increasing force to 48 N, 75 N and 98 N, the friction coefficient increases and encounters more irregularity. This could be due to temperature rise and softening of the alloy resulting in bulk transfer of material to the counterface that is in agreement

with the observations of Laden et al. and Soleymani et al. [42,43].

4. Conclusion

1. The addition of iron to eutectic Al-Si alloys resulted in the formation of plate-like iron-rich intermetallics in the matrix.
2. Higher tendency to microcracking in plate-like intermetallics, leads to the increase of the wear rate of the alloy.
3. The Mn addition to the alloy results to the reduction of the harmful effect of iron due to the formation of the modified alpha intermetallic phases.
4. The addition of Mn to the alloys containing approximately higher than 1.5 wt.% Fe has no impressive influence on the modification of microstructure and does not impede formation of plate-like intermetallic compounds.
5. The wear resistance of 1.6FeMn alloy is higher than the 1Fe alloy despite the presence of plate-like compounds due to the higher hardness of the alloy.

References

[1] J. Clarke and A. D. Sarkar, J. Wear, 54:, 1979, 7.
[2] A. D. Sarkar, J. Wear, 31:, 1975, 331.
[3] D. K. Dwivedi, SHARMA Ashok and T. V. Rajan, J. Trans. Indian Inst. Met.., 54(6):, 2001, 247.
[4] S. A. Kori, B. S. Murty and M. Chakraborty, J. Mater. Sci. Eng., A, 280:, 2000, 94.
[5] M. M. Haque and A. Sharif, J. Mater. Process. Technol., 118:, 2001, 69.
[6] M. Katsuta, K. Oodoshi and S. Kohara, (ICAA-6) (1998), 1945.
[7] N. Saheb, T. Laout, A. R. Daud, M. Harun, S. Radiman and R. Yahaya, J. Wear, 249:, 2001, 656.
[8] J. E. Gruzleski and B. M. Closet, The treatment of liquid aluminium-silicon alloys [M]. Illinois: AFS, 1990.
[9] S. D. Henry, Friction, Lubrication, and Wear Technology ASM Handbook vol. 18 [M]. Met. Park (Ohio): ASM, 1992.
[10] M. Huran, I. A. Talib, A. R. Daud, J. Wear, 194:, 1996, 54.
[11] L. Lasa and J. M. Rodriguez-Ibabe, J. Scr. Mater., 46:, 2002, 477.
[12] F. Cardarelli, Materials Handbook, Common Nonferrous Metals. [M]. New York: Springer, 159.
[13] H. Ye, J. Mater. Eng. Perform., 12:, 2003, 288.
[14] L. G. Hou, H. Cui, Y. H. Cai and J. S. Zhang, J. Mater. Sci. Eng. A, 527:, 2009, 85.
[15] M. Sha, Sh. Wu, X. Wang, L. Wan and P. An, J. Mater. Sci. Eng. A, 535:, 2012, 258.
[16] W. Yuying, L. Xiangfa and B. Xiufang, J. Mater. Charact., 58:, 2007, 205.
[17] J. C. Walker, J. Murray, S. Narania and A. T. Clare, J. Tribol. Lett., 45:, 2012, 49.
[18] C. L. Xu, Y. F. Yang, H. Y. Wang and Q. C. Jian, J. Mater. Sci., 42:, 2007, 6331.
[19] R. Taghiabadi, H. M. Ghasemi and S. G. Shabestari, J. Mater. Sci. Eng. A, 490:, 2008, 162.
[20] B. Dutta, M. Rettenmayr, J. Mater. Sci. Eng. A, 283:, 2000, 218.
[21] S. G. Shabestari and J. E. Gruzleski, J. AFS Trans., 26:, 1995, 285.
[22] S. G. Shabestari, J. Mater. Sci. Eng. A, 383:, 2004, 289.
[23] C. Bidmeshki, V. Abouei, H. Saghafian, S. G. Shabestari and M. T. Noghani, J. Mater. Res. Technol., 5, 3, 2015, 250.
[24] M. S. Probhudev, V. Auradi, K. Venkateswarlu, N. H. Siddalingswamy and S. A. Kori, C Process. Eng. 97:, 2014, 1361.
[25] R. S. Rana, RAJESH Purohit and S. Das, Rev. Int. J. Sci. Res. Publ., 2:, 2012, 1.
[26] W. Yuying, L. Xiangfa, B. Xiufang, J. Mater. Charact., 58:, 2007, 205.
[27] B. Kulunk, S. G. Shabestari, J. E. Gruzleski and D. J. Zuliani, J. AFS Trans., 170:, 1996, 1189.
[28] M. Sha, S. H. Wu, X. Wang, L. Wan and P. J. An, Mater. Sci. Eng. A, 535:, 2012, 258.
[29] A. Hekmat-Ardakan, F. Ajersch and X-G. Chen, J. Mater. Sci., 46:, 2011, 2370.
[30] X. F. WU, G. A. Zhang, J. Mater. Sci., 46:, 2011, 7319.
[31] A. M. Samuel, F. H. Samuel and H. W. DOTY, J. Mater. Sci., 31:, 1996, 5529.
[32] M. Tash, F. H. Samuel, F. Mucciardi and H. W. Doty, J. Mater. Sci. Eng. A, 443:, 2007,185.
[33] M. Warmuzek, W. Ratuszek and G. Sek-Sas, J. Mater. Charact., 54:, 2005, 31.
[34] C-L. Chen, R. C. Thomson, J. Intermetallics, 18:, 2010, 1750.
[35] L. F. Mondolfo, Aluminum alloys: structure and properties M. London: Butterworth, 1978.
[36] V. Abouei, H. Saghafian, SH. Kheirandish, J. Wear, 262, 2007, 1225.
[37] C. Bidmeshki, A. Shokuhfar and V. Abouei, J. Metall. Res. Technol., 113, 2015, 203.
[38] N. A. Belov and A. A. Aksenov, Iron in Aluminum Alloys: impurity and alloying element New York: Taylor and Francis, 2002.
[39] M. H. Mulazimoglu, A. Zaluska, J. E. Gruzleski and F. Paray, J. Met. Mater. Trans., 1996, 27A: 929.
[40] P. Ashtari, H. Tezuka and T. Sato, J. Mater. Trans., 44, 2003, 2611.
[41] T. O. Mbuya T O, B. O. Odera and S. P. Nganga, Rev. Int. J. Cast Met. Res., 16, 2003, 1.
[42] K. Laden, J. D. Gu'erin, M. Watremez and J. P. Bricout, J. Tribol. Lett., 8, 2000, 237.
[43] S. Soleymani, A. Abdollah-Zadeh and S. AhmadAlidokht, J. Surf. Eng. Mater. Adv. Technol., 1, 2011, 95.